Cellular Physiology and Biochemistry

Cell Physiol Biochem 2018;46:9-22

DOI: 10.1159/000488404

Published online: March 23, 2018

Accepted: January 16, 2018

Original Paper

Cardiac-Specific Overexpression of Silent Information Regulator 1 Protects Against Heart and Kidney Deterioration in Cardiorenal Syndrome via Inhibition of Endoplasmic Reticulum Stress

Dong Huang[a] Mei-ling Yan[a] Kan-kai Chen[a] Rong Sun[a] Zhi-feng Dong[a] Peng-long Wu[a] Shuai Li[a] Guang-shuo Zhu[b] Shi-xin Ma[a] Ye-sheng Pan[a] Jing-wei Pan[a] Wei Zhu[c] Jun Xu[d] Meng Wei[a] Jing-bo Li[a]

[a]Heart Center, Shanghai Jiaotong University Affiliated Sixth People's Hospital, Shanghai Jiaotong University School of Medicine, Shanghai, P. R. China, [b]Division of Cardiology, Johns Hopkins Medical Institutions, Baltimore, Maryland, U.S.A, [c]Cardiovascular Key Laboratory of Zhejiang Province, the Second Affiliated Hospital, Zhejiang University School of Medicine, Hangzhou, P. R. China, [d]Department of Anesthesia, University of Iowa Hospitals and Clinics, Iowa City, Iowa, U.S.A

Key Words

Cardiorenal syndrome • Genetically Altered and Transgenic Models • Myocardial Infarction • Nephrology and Kidney • Remodeling

Abstract

Background/Aims: Increased endoplasmic reticulum (ER) stress contributes to development of cardiorenal syndrome (CRS), and Silent Information Regulator 1 (SIRT1), a class III histone deacetylase, may have protective effects on heart and renal disease, by reducing ER stress. We aimed to determine if SIRT1 alleviates CRS through ER stress reduction. ***Methods:*** Wild type mice (n=37), mice with cardiac-specific SIRT1 knockout (n=29), or overexpression (n=29), and corresponding controls, were randomized into four groups: sham MI (myocardial infarction) +sham STNx (subtotal nephrectomy); MI+sham STNx; sham MI+STNx; and MI+STNx. To establish the CRS model, subtotal nephrectomy (5/6 nephrectomy, SNTx) and myocardial infarction (MI) (induced by ligation of the left anterior descending (LAD) coronary artery) were performed successively to establish CRS model. At week 8, the mice were sacrificed after sequential echocardiographic and hemodynamic studies, and then pathology and Western-blot analysis were performed. ***Results:*** Neither MI nor STNx alone significantly influenced the other healthy organ. However, in MI groups, STNx led to more severe cardiac structural and functional deterioration, with increased remodeling, increased BNP levels, and decreased EF, Max +dp/dt, and Max -dp/dt values than in sham MI +STNx groups. Conversely, in STNx groups, MI led to renal structural and functional deterioration, with more severe morphologic changes, augmented desmin and decreased nephrin expression, and increased BUN, SCr and

D. Huang, M.-L. Yan and K.-K. Chen contributed equally to this study.

Professor Meng Wei, M.D
and Jing-bo Li, M.D.

Heart Center, Shanghai Jiaotong University
Affiliated Sixth People's Hospital, 600 Yishan Road, Shanghai, 200233 (China)
Tel. (+86)-21-24058334, E-Mail mrweei@medmail.com.cn, lijb@sjtu.edu.cn

UCAR levels. In MI+STNx groups, SIRT1 knockout led to more severe cardiac structural and functional deterioration, with higher Masson-staining score and BNP levels, and lower EF, FS, Max +dp/dt, and Max -dp/dt values; while SIRT1 overexpression had the opposite attenuating effects. In kidney, SIRT1 knockout resulted in greater structural and functional deterioration, as evidenced by more severe morphologic changes, higher levels of UACR, BUN and SCr, and increased desmin and TGF-β expression, while SIRT1 overexpression resulted in less severe morphologic changes and increased nephrin expression without significant influence on BUN or SCr levels. The SIRT1 knockout but not overexpression resulted in increased myocardial expression of CHOP and GRP78. Cardiac-specific SIRT1 knockout or overexpression resulted in increased or decreased renal expression of CHOP, Bax, and p53 respectively. ***Conclusions:*** Myocardial SIRT1 activation appears protective to both heart and kidney in CRS models, probably through modulation of ER stress.

Introduction

Cardiac and renal diseases share several risk factors, and are physiologically interlinked. Although physicians have long recognized that dysfunction of either heart or kidney seldom occurs in isolation, only recently has the concept of the cardiorenal syndrome (CRS), along with a classification system, been proposed [1]. Studies have shown close heart-kidney interactions, for example chronic kidney dysfunction (CKD) increases risk for cardiovascular events, and patients with chronic heart failure (CHF) and microalbuminuria or CKD have worse outcomes than those with CHF alone [2-4]. However, the underlying mechanisms remain poorly understood and therapeutic options are limited.

Hemodynamic changes are probably the most evident contributors to heart-kidney interactions. Other mechanisms implicated in CRS pathogenesis include sympathetic over-activity, renin-angiotensin-aldosterone axis changes, oxidative injury and endothelial dysfunction, anemia, inflammation and obesity [5]. Furthermore, we have shown that myocardial infarction (MI) worsened glomerular injury and microalbuminuria in rats with pre-existing renal impairment, with a crucial role being played by activation of endoplasmic reticulum (ER) stress [6, 7].

Silent Information Regulator 1 (SIRT1), a nuclear and cytoplasmic class III histone deacetylase, regulates a wide variety of cellular processes [8, 9]. *In vitro* and *in vivo* studies have shown that: (1) SIRT1 activation was protective of cardiac and renal function under stress conditions [10, 11], (ii) SIRT1 deficiency was associated with pathophysiologic changes in cardiovascular and renal disease [11, 12], and (3) SIRT1 attenuated ER stress in both heart and kidney [13, 14].

We hypothesized that the protective effect of SIRT1 on cardiac and renal function is effected through its modulation of ER stress. We tested this hypothesis by using genetically altered mice, in which cardiac expression of SIRT1 was either upregulated or downregulated in CRS models, to investigate if the protective effect of SIRT1 on cardiac and renal function is through its modulation of ER stress.

Materials and Methods

Animal preparation

In our study we used four types of male mice: (1) wild type (WT) C57BL/6 (Experimental Animal Center, Fudan University, Shanghai, China), (2) cardiac-specific SIRT1 knockout (CKO), (3) cardiac-specific SIRT1 pre-overexpression transgenic (Tg), and (4) their corresponding control littermates (Shanghai Biomodel Organism Science and Technology Development Co., Ltd).

Mice were acclimatized for two weeks before the start of the experiment, in the same housing used during the experiments, namely a pathogen-free facility under controlled temperature (24 ± 2°C) and

humidity (50 ± 5%), with a 12-hour light/dark cycle. At the start of the experiments, mice were 8-10 weeks of age and weighed 18-22g. The animal research study protocols complied with the guide for the care and use of laboratory animals published by the National Institutes of Health in the USA, and were approved by the Animal Care Committee of Shanghai Sixth Hospital, Shanghai Jiaotong University School of Medicine in China.

Experimental protocols

1. Creation of transgenic mouse model (cardiac-specific SIRT1 knockout or overexpression). To generate cardiac-specific SIRT1-knockout mice, mice carrying a floxed Sirt1 allele ($Sirt1^{flox/flox}$; Jackson Laboratory), (in which exon 4 of Sirt1 was flanked by loxP sites), were crossed with Myh6-Cre^{+} transgenic mice (B6. FVB(129)-Tg (Myh6-cre/Esr1*) 1Jmk/JSmoc, (Shanghai Biomodel Organism Science and Technology Development Co., Ltd, Shanghai, China) expressing Cre recombinase under the control of the Myh6 promoter. Genotyping was confirmed by PCR from genomic DNA prepared from tail biopsies. All mice were kept on a full C57BL/6 background.

For the detection of Sirt1 protein, we firstly used a monoclonal antibody produced by immunizing rabbit with a synthetic peptide corresponding to residues surrounding Phe297 of human Sirt1 protein, according to the manufacturer's instructions (Cell Signalling, Beverly, MA, USA. #9475, species reactivity: human, mouse, rat, monkey), which may also recognize the region encoded by exon 4 of mouse Sirt1 (aa 256-306). Secondly, although deletion of exon 4 should result in expression of a truncated form of sirt1 with similar molecular weight, several studies with similar Sirt1 knockout mice models, (generated by in-frame deletion of exon 4), have shown that the cardiac expression of Sirt1 was significantly reduced, while the epitopes of Sirt1 antibodies were not clearly stated [15, 16]. Lastly, to confirm the deletion of exon 4, we performed quantitative RT-PCR analyses using total RNA prepared from cardiac tissue, using primer specific for exon 4. The results showed that the expression of full-length Sirt1 (with exon 4) was significantly reduced in the Sirt1 KO group compared to the control group.

The model for overexpression of Sirt1 was created through intramyocardial injection of lentivirus vectors containing sirt1 cDNA (Hanbio, Shanghai, China). Viral supernatant was generated by 293FT cells transfected with EX-Lv105 plasmid and lentiviral packaging plasmids. Viral titers were determined with a quantity kit. The C57BL/6 mice were anesthetized by intraperitoneal injection of pentobarbital (50mg/kg) followed by intubation and mechanical ventilation with room air. A thoracotomy was performed at the left fourth intercostal space to expose the anterior left ventricular (LV) wall. A total volume of 20 μl virus containing solution (1×10^{8} pfu/ml) was injected into four different sites (5 μl each) around the anterior LV wall, through a sterile Hamilton syringe with a 30-gauge sterile beveled needle, under visual guidance. The syringe was held in place until the bleb formed by the solution disappeared. Then the needle was removed, and the chest wall was closed.

2. Experimental groups. The mice of each of the WT, CKO, and Tg lines (see "Animal Preparation" above) were randomized into four procedure groups: (1) sham MI + sham STNx; (2) MI + sham STNx; (3) sham MI + STNx; and (4) MI + STNx (MI, myocardial infarction; STNx, subtotal nephrectomy).

3. Procedures to induce chronic renal dysfunction and myocardial infarction. We initially generated a model of subtotal nephrectomy (5/6 nephrectomy, SNTx). Four weeks later, MI was induced. After a further four weeks, we conducted echocardiographic and hemodynamic studies, and then the mice were sacrificed and their tissues harvested for histopathology and immunohistochemistry, ELISA, and Western-blot studies.

Induction of chronic renal dysfunction

A subtotal nephrectomy to create a model of chronic renal dysfunction (STNx) or a sham operation, was performed on eight-week old WT, KO and Tg mice. The STNx was accomplished by a two-step surgical procedure, with an interval of one week between the steps; for each step the mice were anesthetized by intraperitoneal injection of pentobarbital (50mg/kg), [17]. In the first step, two to three arterial branches of the left kidney were ligated, leaving an intact kidney segment. In the second step, the right kidney was removed. Thereafter, the mice received 0.9% NaCl in their drinking water. The sham STNx mice received similar skin incisions and sutures in one week apart.

To confirm kidney injury before sacrifice, serum and urine samples were collected to assess changes in blood urea nitrogen (BUN), serum creatinine (SCr), and urinary albumin to creatinine ratio (UACR).

Induction of myocardial infarction

Four weeks after the STNx or sham STNx operation, we performed a left anterior descending (LAD) ligation or sham-ligation [18]. Briefly, anesthesia was induced with isofurane (2% for 6-8 mins), and the depth of anesthesia was monitored by tail pinch reflex. Mice were intubated with a 22f tube, and ventilated with a rodent ventilator (model 687; Harvard Apparatus Inc., MA, USA) at 100 breaths/min with room air. The mice were kept warm with heat lamps. Rectal temperature was monitored, and maintained between 36°C and 37°C. The chest was opened by a horizontal incision at the third intercostal space. Heart exposure was performed by a thoracotomy at the fourth left intercostal space. After removing the pericardial sac, MI was induced by ligating the LAD branch of the left coronary artery with an 8-0 Prolene suture, with silicon tubing (1 mm outer diameter) placed on top of the LAD coronary artery, 2 mm below the border between the left atrium (LA) and left ventricle (LV). Ischemia was confirmed by electrocardiogram (ECG) change (lead II, ST elevation). After LAD ligation, the rib space, overlying muscles, and skin were closed. When recovered from anesthesia, the mice were extubated and returned to their cages. The mice were then housed in a climate-controlled environment for four weeks. The sham MI mice received only a similar procedure of chest opening and closure without ligation of LAD.

Transthoracic Echocardiography

Transthoracic echocardiographic (TTE) examination was performed, four weeks after the induction of MI, using a Vevo 2100 micro imaging system with a MS400 30-MHz linear array transducer (VisualSonics Inc., Toronto, Canada). For the TTE procedure, mice were anesthetized by intraperitoneal injection of pentobarbital sodium (50 mg/kg), and placed supine on a platform with a heating unit to maintain their body temperature at 37.0±0.5°C. Heart rate (HR) was continuously monitored by ECG electrodes. Both para-sternal long-axis and short-axis views were performed. The M-mode from the long axis view was obtained to measure increased interventricular septal (IVS) thickness, and the M-mode from the short axis view was performed to measure thickness of LV anterior wall (LVAW), LV posterior wall (LVPW), LV end-diastolic diameter (LVEDD), and the LV end-systolic diameter (LVESD). End-diastolic and end-systolic measurements were obtained at the time of maximal and minimal internal chamber dimensions, respectively. In addition, LV ejection fraction (EF) value, fractional shortening (FS), and LV mass were calculated, as previously described [19]. All measurements were repeated thrice from at least 10 consecutive cardiac cycles, and were analyzed by a single observer blinded to the treatment protocol, according to the recommendations of the American Society of Echocardiography [17, 20]. The mean values were used for data analysis.

Hemodynamic measurement

Four weeks after the induction of MI, all mice were anesthetized with isofurane, intubated and ventilated for cardiac catheterization procedures [21]. The mice were placed supine on a platform with a heating unit. The body temperature was maintained at 37.0±0.5°C to minimize heart rate variation. The right carotid artery was cannulated with a 1.2F pressure catheter (Transonic, Ithaca, NY, USA), which was passed retrogradely into the LV. The LV pressure tracings were digitized with a PowerLab physiological recorder (AD Instruments, Australia), and stored in a computer for off-line analysis. Left ventricular end-diastolic pressure (LVEDP), the maximum/minimum first derivative of LV pressure over time ($\pm dP/dt_{max}$), and mean arterial pressure (MAP), were analyzed in a blinded fashion, with dedicated software (LabChart 8).

Sample collection

To monitor urinary volume change, 24 hr urine samples were collected, by using the metabolism cage, at baseline and every four weeks from the beginning of the study. Urine samples were stored at -20°C. Urinary albumin and creatinine concentrations were measured with assay kits (Shibayagi, Japan). The urinary albumin to creatinine ratio (UACR) was calculated by using a formula based on albumin and creatinine levels.

After taking the hemodynamic measurements, blood samples were collected (under anesthesia by intraperitoneal injection of pentobarbital sodium (50 mg/kg)), and the enterocoelia were cut off to expose the inferior vena cava. The blood samples were collected in heparinized microtubes and centrifuged at 3000r/s for 15 mins (3K30, Sigma, USA). The SCr, and BUN levels were measured using the enzymatic method. Plasma brain natriuretic peptide (BNP) was measured with an AssayMaz mouse BNP-45 (mBNP-45) assay kit (Phoenix Pharmaceuticals, Inc, CA, USA).

Histological Examination and Immunohistochemistry

Four weeks after the MI surgery, all mice were sacrificed by injection of pentobarbital sodium (50 mg/kg). Immediately after collection of a plasma sample from the inferior vena cava (as mentioned in sample collection), the chest was opened. The LV of the heart and left residual kidney were collected and weighed. Tissues were cut in half; one half was snap frozen in liquid nitrogen for western-blot (see below), the other half was fixed in neutral buffered formalin, and processed for histopathology and immunohistochemistry.

Among the second half of collected tissue samples, half of them were then homogenized in 10% buffered paraformaldehyde, and processed for hematoxylin-eosin (HE) or Masson dye staining. Tissue sections (1μm thick) were stained by Mallory and viewed using a light microscope (Leica, Frankfurt, Germany) with a computer-assisted analyzer (Image Pro Express system, USA). Focal interstitial fibrosis was defined as an increase in matrix deposition in interstitial spaces that was distinguishable from the surrounding area (perivascular areas were excluded).

Immunohistochemistry was used to assess desmin, TGF-β1, and nephrin expression in the kidney. Tissues were fixed with 10% paraformaldehyde and embedded in paraffin, sectioned into 4 μm-thick slices, and stained with periodic acid-Schiff reagent. Immunohistochemistry was performed as previously described [22], using a primary antibody against desmin, TGF-β1 and nephrin (Abcam, Cambridge, United Kingdom), followed by the Nichirei simple stain kit (Nichirei, Messe Düsseldorf, Germany). Immunological changes were quantified by positive diaminobenzidine staining, with scoring from 0 to 5 by double-blinded histologists.

Enzyme linked immunosorbent assay (ELISA)

Blood was collected in heparinized microtubes rapidly after exposure of the inferior vena cava and subjected to centrifugation (3000r/s) (Sigma, USA). The three immunosorbent plasma assays performed were BNP (mBNP-45, ASSAYPRO, USA), UACR, and BUN using the enzymatic method by Sirolimus.

Western-blot

For immune-blot analysis, heart and kidney samples were homogenized in lysis buffer (50 mmol/L Tris-HCl, pH 7.4, 0.1% sodium dodecyl sulfate, 1% Igepal CA-630, 0.15 mol/L NaCl, 0.25% Na-deoxycholate, and 1 mmol/L EDTA supplemented with protease inhibitors). Cardiac and renal cortical tissue (30 mg) was homogenized with 1 ml of modified RIPA buffer in the presence of protease and phosphatase inhibitors. Equal amounts of protein (30μg) were separated by 10% SDS-PAGE, and electrophoretically transferred to nitrocellulose membranes (Amersham Biosciences, Piscataway, NJ, USA). Western-blot analysis was performed with specific antibodies as per the manufacturer's protocol. Antibodies used to assess ER stress in heart and kidney were directed at CHOP, GRP78, p53, and BAX. As controls we used tubulin, GAPDH (Cell Signal Technology), and β-actin (Calbiochem, Germany).

Statistical Analysis

Statistical analysis was performed using SPSS 13.0 for Windows (SPSS Inc, Chicago, USA). Continuous variables were expressed as mean ± SEM, and were compared using the *t*-test. For comparisons among multiple groups, we used one- or two-way ANOVA and Bonferroni post-test. A two-tailed *P* value of < 0.05 was considered statistically significant.

Results

Greater structural and functional deterioration of the heart and kidney after concomitant injuries vs. isolated injury

Compared with the MI+ sham STNx group, the MI + STNx group showed significantly lower EF (31.97±10.7% vs. 46.31±12.3%, P<0.05) (Table 1), Max +dp/dt (5158.8±687.4 vs. 7888.5±987.6 mmHg/s, P<0.05) (Table 2) and Max -dp/dt (-3515.8±431.7 vs. -5917.64±775.3 mmHg/s, P<0.05) (Table 2), indicating worsened cardiac remodeling in the MI + STNx group. A significant remodeling of cardiac tissue seen in H&E staining (Fig. 1 B), and a higher mean score for Masson staining of the heart (6.23±1.02 vs. 5.5±0.79, P<0.05) was also observed in MI + STNx group than in the MI + sham STNx group (Fig. 1 A, C), indicating a higher degree of fibrosis in the MI +STNx compared group to the MI + sham STNx group. These changes were

further supported by a significantly higher BNP level after concomitant cardiac and renal injury in the MI +STNx group compared to the MI + sham STNx group (655.43±149.74 pg/ml vs. 517.71±120.63 pg/ml, P<0.05) (Fig. 1D).

In the MI + STNx group compared to the sham MI + STNx group, the residual kidney showed greater degree of glomerular swelling, mesangial hyperplasia, and disintegration with cristae in podocytes (Fig. 2 A); and a higher degree of renal fibrosis, and higher levels of desmin, TGF-b1, BUN, SCr and UACR, and significantly lower levels of nephrin (Fig. 2 A-L). However, induction of MI alone did not affect renal structure or function in mice without STNx four weeks post-MI. Furthermore, STNx alone had no significant influence on cardiac structure and function.

Cardiac-specific overexpression of SIRT1 protected both the heart and the kidney in CRS

After induction of both MI and STNx, the SIRT1 knockout (KO) mice had: (1) significantly lower EF (26.94±8.6% vs. 31.97±10.7%, P<0.05) and FS (12.36±3.1% vs. 26.26±4.3%, P<0.05),

Table 1. Echocardiographic parameters assessed at eight weeks post-procedures in four experimental groups of WT mice. LVEDD, left ventricular end-diastolic dimension; LVESD, left ventricular end-systolic dimension; LVPW, left ventricular posterior wall thickness; EF, ejection fraction; FS, fractional shortening; LV mass, left ventricular mass index. Values are mean±SEM. * P<0.05 versus Sham MI + Sham STNx; §P<0.05 versus MI + Sham STNx. All results from WT mice

	Sham MI+Sham STNx (n=10)	MI+Sham STNx (n=8)	Sham MI+STNx (n=9)	MI+STNx (n=10)
LVEDD (mm)	2.95±0.37	3.54±0.38*	2.98±0.38	4.06±0.44
LVESD (mm)	1.52±0.18	2.18±0.32*	1.68±0.32	2.99±0.39
LVPW (mm)	0.66±0.13	0.64±0.12	0.64±0.12	0.39±0.15
EF (%)	76.32±13.2	46.31±12.3*	73.31±12.3	31.97±10.7§
FS (%)	48.46±9.6	28.36±5.6*	47.36±5.6	26.26±4.3
LV mass (mg)	55.99±12.5	71.75±15.6*	58.75±15.6	73.29±20.4
LV mass (corrected) (mg)	44.79±9.8	57.39±13.8*	46.39±13.8	58.63±15.9
Heart rate (beats/min)	438.8±39.5	457.0±47.8	457.0±47.8	455.8±43.2

Table 2. Hemodynamic parameters assessed at eight weeks post-procedures in the WT mice. EDP, LV end diastolic pressure; Max dP/dt, the maximal rate of pressure rise; Max -dP/dt, the maximal rate of pressure fall. * P<0.05 versus Sham MI + Sham STNx; §P<0.05 versus MI + Sham STNx. All results from WT mice

	Sham MI+Sham STNx (n=10)	MI+Sham STNx (n=8)	Sham MI+STNx (n=9)	MI+STNx (n=10)
Max pressure (mmHg)	110.2±23.8	107.5±19.8	108.5±19.8	94.2±14.3
EDP (mmHg)	3.71±1.03	4.57±1.27*	4.27±1.17	3.37±0.68
Heart rate (beats/min)	494.3±58.9	450.8±27.6	480.8±24.6	403.8±35.7
Max dP/dt (mmHg/s)	12025.6±1578.9	7888.5±987.6*	11888.5±1287.6	5158.8±687.4§
Max -dP/dt (mmHg/s)	-9372.0±877.6	-5917.6±775.3*	-8917.6±795.3	-3515.8±431.7§

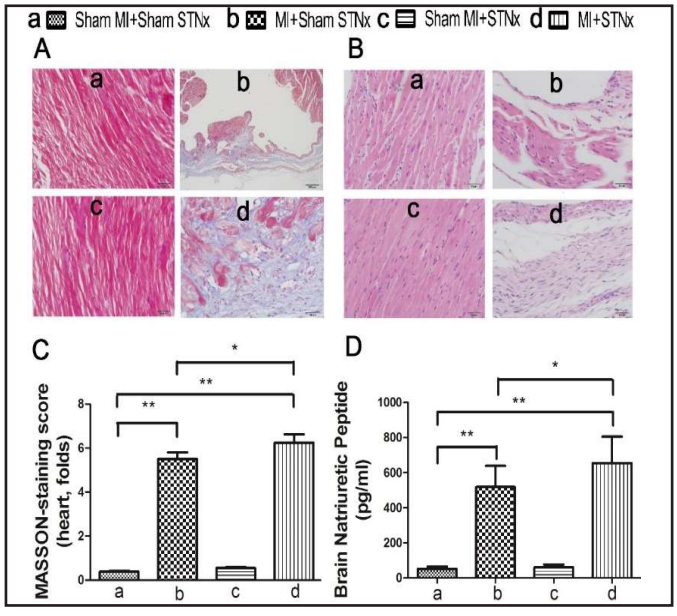

Fig. 1. Representative images of heart histology and level of brain natriuretic peptide before and after procedures. A: Cardiac pathological section with Masson staining; B: Cardiac pathological section with HE staining; C: Masson-staining score of heart; D: BNP level. Brain natriuretic peptide (BNP). *P<0.05, ** p<0.01, n=7 for each group, all results from WT mice.

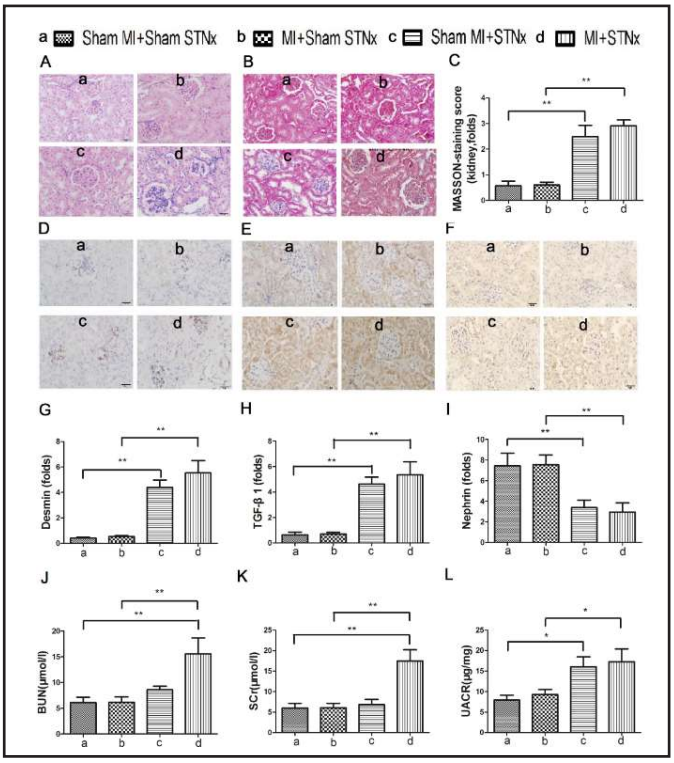

Fig. 2. Representative images of renal histology and level of kidney function before and after procedures. A: Pathological section with HE staining post MI; B: Pathological section with Masson staining post MI; C: Masson-staining score of kidney post MI and MI + STNx; D: Immunohistochemistry of Desmin in kidney; E: Immunohistochemistry of TGF-β1 in kidney; F: Immunohistochemistry of Nephrin in kidney; G: Desmin score; H: TGF-β1 score; I: Nephrin score; J: Blood urea Nitrogen (BUN) level; K: Serum creatinine (Scr) level; L: Urinary albumin to creatinine ratio (UACR). * P<0.05, ** P<0.01, n=7 for each group, all results from WT mice.

Table 3. Echocardiographic data from KO, Tg, and corresponding control mice after the procedures. LVEDD, left ventricular end-diastolic dimension; LVESD, left ventricular end-systolic dimension; LVPW, left ventricular posterior wall thickness; EF, ejection fraction; FS, fractional shortening; LV Mass, left ventricular mass index. Values are mean±SEM. * P<0.05 ** p<0.01versus KO control MI + Sham STNx; §P<0.05 versus KO control MI + STNx; Ł P<0.05 versus Tg control MI + Sham STNx; ‡P<0.05 versus Tg control MI + STNx

	KO					Tg					
	control Sham MI+ Sham STNx (n=10)	control MI+ Sham STNx (n=9)	control MI+ STNx (n=10)	Sham MI+ Sham STNx (n=10)	MI+ Sham STNx (n=10)	MI+ STNx (n=9)	control Sham MI+ Sham STNx (n=10)	control MI+ Sham STNx (n=10)	control MI+ STNx (n=10)	Sham MI+ Sham STNx (n=10)	MI+ Sham STNx (n=9)	MI+ STNx (n=10)
LVEDD (mm)	2.95±0.37	3.54±0.38	4.06±0.44	2.98±0.38	4.88±0.57**	4.22±0.37	2.91±0.35	3.58±0.35	4.16±0.44	2.99±0.24	3.43±0.23	4.04±0.42
LVESD (mm)	1.52±0.18	2.18±0.32	2.99±0.39	1.51±0.11	4.02±0.45**	3.69±0.32§	1.51±0.19	2.16±0.36	2.89±0.36	1.58±0.17	2.68±0.24Ł	2.59±0.36
LVPW (mm)	0.66±0.13	0.64±0.12	0.39±0.15	0.65±0.09	0.59±0.18	0.43±0.12	0.63±0.12	0.68±0.11	0.38±0.17	0.69±0.15	0.61±0.65	0.45±0.17
EF (%)	76.32±13.20	46.31±16.30	31.97±10.70	74.38±8.60	36.71±12.70*	26.94±8.60§	76.48±13.90	46.34±12.56	31.57±10.89	71.78±9.60	48.24±12.50	39.39±8.80‡
FS (%)	48.46±9.60	28.36±5.60	26.26±4.30	49.66±7.78	17.67±3.50**	12.36±3.10§	48.54±9.90	28.3±5.80	26.45±4.50	45.76±8.18	32.85±3.80Ł	29.86±2.60‡
LV mass (mg)	55.99±12.50	71.75±15.60	73.29±20.40	54.32±8.94	104.52±25.20*	64.69±15.80	55.45±12.60	71.7±15.20	73.49±20.34	54.71±6.97	65.14±12.60	83.96±28.90
LV mass (corrected) (mg)	44.79±9.80	57.39±13.80	58.63±15.90	45.37±7.92	83.21±19.80*	51.75±12.10	44.98±9.60	57.4±13.30	58.54±15.77	44.35±6.71	52.11±8.90	69.16±19.70
Heart rate (beats/min)	438.8±39.5	457±47.8	455.8±43.2	453±46.9	446.7±29.6	475.9±48.8	438.5±39.9	456.45±47.3	455.45±43.3	464±49.7	447.6±43.1	465.3±26.4

(2) significantly greater LVESD (3.69±0.32mm vs. 2.99±0.39mm, P<0.05)(Table 3), along with (3) significantly lower Max +dp/dt (3425.6±403.8 mmHg/s vs. 5158.8±687.4mmHg/s, P<0.05) and Max -dp/dt (-2986.5±169.5mmHg/s vs. -3515.8±431.7mmHg/s, P<0.05, Table 4), indicating worsened cardiac remodeling in the SIRT1 KO MI + STNx group compared with the KO control MI +STNx group. A significant remodeling in heart H&E staining (Fig. 3 B), and higher score for Masson staining of the heart (8.82±0.96 vs. 5.71±1.62, P<0.05) was also observed in SIRT1 knockout group (Fig. 3 A, C), indicating a higher degree of fibrosis in the SIRT1 KO MI + STNx group compared to the KO control MI + STNx group. These changes were further supported by a significantly higher BNP level (631.43±142.99pg/ml vs. 498.43±93.16pg/ml, P<0.05) (Fig. 3 D) in the SIRT1 KO MI + STNx group compared to the KO control MI + STNx group.

In contrast, the SIRT1 overexpression group had attenuated cardiac remodeling and fibrosis, as evidenced by significantly increased EF (39.39±8.8% vs. 31.57±10.89%, P<0.05), and FS (29.86±2.6% vs. 26.45±4.5%, P<0.05) (Table 3), along with a significantly lower BNP level (BNP: 368.43±46.61pg/ml vs. 470.14±97.17pg/ml, P<0.05, Fig. 3 D) and Masson score (4.34±1.34 vs. 5.43±1.81, P<0.05, Fig. 3 A), after induction of both MI and STNx compared with the WT control group that had undergone the same operations.

Table 4. Hemodynamic parameters in KO, Tg, and corresponding control mice after procedures. EDP, LV end diastolic pressure; Max dP/dt, the maximal rate of pressure rise; Max -dP/dt, the maximal rate of pressure fall. * P<0.05 ** p<0.01versus KO control MI + Sham STNx; §P<0.05 versus KO control MI + STNx; Ł P<0.05 versus Tg control MI + Sham STNx; ‡P<0.05 versus Tg control MI + STNx

	KO						Tg					
	control Sham MI+ Sham STNx (n=10)	control MI+ Sham STNx (n=9)	control MI+ STNx (n=10)	Sham MI+ Sham STNx (n=10)	MI+ Sham STNx (n=10)	MI+ STNx (n=9)	control Sham MI+ Sham STNx (n=10)	control MI+ Sham STNx (n=10)	control MI+ STNx (n=10)	Sham MI+ Sham STNx (n=10)	MI+ Sham STNx (n=9)	MI+ STNx (n=10)
Max pressure (mmHg)	110.16±23.80	107.5±19.80	94.2±14.30	98.34±11.57	85.3±16.70*	79.89±18.60§	110.36±23.40	105.4±19.56	93.12±14.13	99.74±12.47	86.4±15.30	81.3±16.90
EDP (mmHg)	3.71±1.03	4.57±1.27	3.37±0.68	4.26±0.85	4.47±1.28	4.32±1.37§	3.74±1.07	4.83±1.25	3.27±0.58	3.96±0.65	3.94±0.85	4.02±1.36
Heart rate (BPM)	494.31±58.90	450.8±27.60	403.77±35.70	463.7±38.90	446.3±26.80	452.6±43.10	495.1±58.40	450.28±27.16	421.65±35.26	473.1±48.30	470.2±49.70	446.3±51.30
Max dP/dt (mmHg/s)	12025.6±1578.9	7888.5±987.6	5158.8±687.4	11543±1326.5	5083.8±456.7*	3425.6±403.8§	12043.6±1588.9	7838.5±967.2	5149.8±676.3	10943±1021.5	8117.5±1004.7Ł	5672.9±677.5‡
Max -dP/dt (mmHg/s)	-9372.03±877.6*	-5917.64±775.3	-3515.8±431.7	-8872.53±865.6	-4066.7±692.4*	-2986.5±169.5§	-9467.03±856.6*	-5934.14±764.3	-3537.8±434.7	-8761.5±786.3	-6543.2±897.4Ł	-4788.9±768.4‡

In the residual kidney, the CKO group showed a higher degree of glomerular swelling, mesangial hyperplasia, and disintegration with cristae in podocytes, compared to their WT control group in H&E staining (Fig. 4 A), and a significantly higher Masson-staining score (7.43±1.37 vs 3.35±1.13, P<0.01) (Fig. 4 B), indicating a greater extent of renal cortical fibrosis in the CKO group (Fig. 4 B). Significantly increased expression of desmin and TGF-β1 (7.01±0.89 vs. 5.2±1.10, P<0.05; 5.97±0.82 vs. 5.48±1.03, P<0.05, respectively) (Fig. 5 A-D), along with significantly decreased expression of nephrin (0.71±0.17 vs. 3.08±0.69, P<0.05) were also present in the CKO MI+ STNx group compared with CKO control MI + STNx group (Fig. 5 E,F). In terms of renal function, the SIRT1 knockout group showed significantly increased BUN (19.31±2.29 vs. 15.88±1.69 μmol/l, P<0.05), SCr (21.27±2.05 vs. 18.6±0.77 μmol/l, P<0.05), and UACR (22.03±1.56μg/mg vs. 15.67±1.16 μg/mg, P<0.05) levels in the CRS model compared with control group (Fig. 4 D-F).

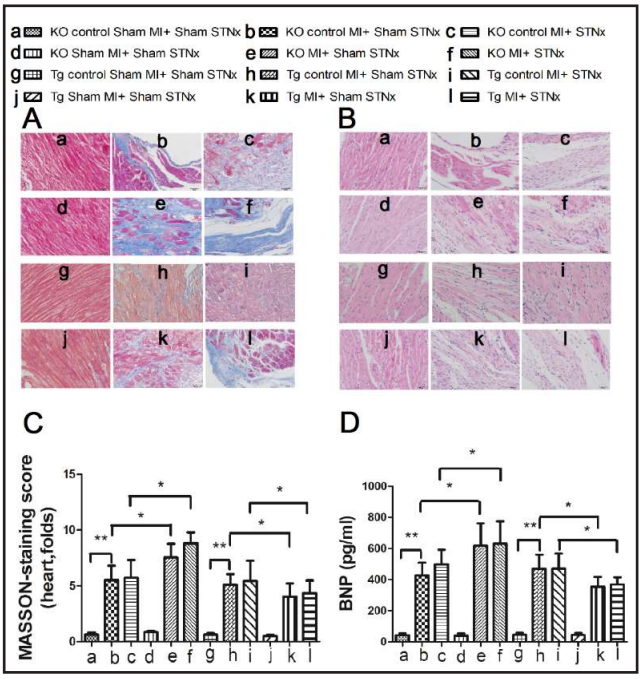

Fig. 3. Effect of SIRT1 on the heart histology and level of brain natriuretic peptide before and after procedures. A: Pathological section with Masson staining; B: Pathological section with HE staining; C: Masson-staining score of heart; D: BNP level. *P<0.05, ** P<0.01, n=7 for each group.

In contrast, the kidney in mice in the SIRT1 overexpression group, presented with significantly less severe renal structural and functional alteration after induction of both MI and STNx, as evidenced by lower Masson score (2.84±0.43 vs. 3.38±0.59, P<0.05) (Fig. 4 B), increased expression of desmin and TGF-β1 (5.51±0.43 vs. 3.01±0.72, P<0.05; 5.81±0.87 vs. 3.96±0.92, P<0.05, respectively) (Fig. 5 A-D), and decreased UCAR (13.91±1.44 vs. 17.81±1.53 μg/mg, P<0.05, Fig. 4 F) compared with the Tg control MI + STNx group. However, BUN (14.69±1.88 vs. 15.59±1.11, P>0.05) and SCr (15.00±1.68 vs. 17.48±1.52, P>0.05) were not significantly altered by overexpression of SIRT1 (Fig. 4 D, E).

ER stress is involved in CRS and modulated by SIRT1

We evaluated the activation of ER stress in both the heart and the kidney through detection of four proteins. In groups that had undergone both MI and STNx, the CKO group showed significantly higher levels of CHOP and GRP78 expression within the myocardium than did the related WT control group (2.59±0.37 vs. 1.53±0.29, P<0.05; 3.17±0.36 vs. 1.96±0.28, P<0.05, respectively) (Fig. 6 A-D). In contrast, SIRT1 overexpression within the

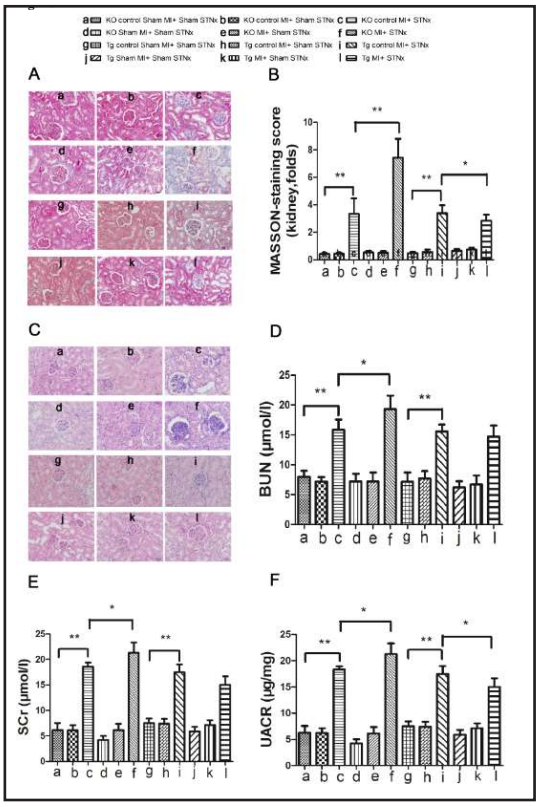

Fig. 4. Effect of SIRT1 on the renal histology and function before and after procedures. A: Pathological section with Masson dying; B: Masson-staining score; C: HE staining of kidney; D: BUN level; E: SCr level; F: UACR level. *P<0.05, ** P<0.01, n=7 for each group.

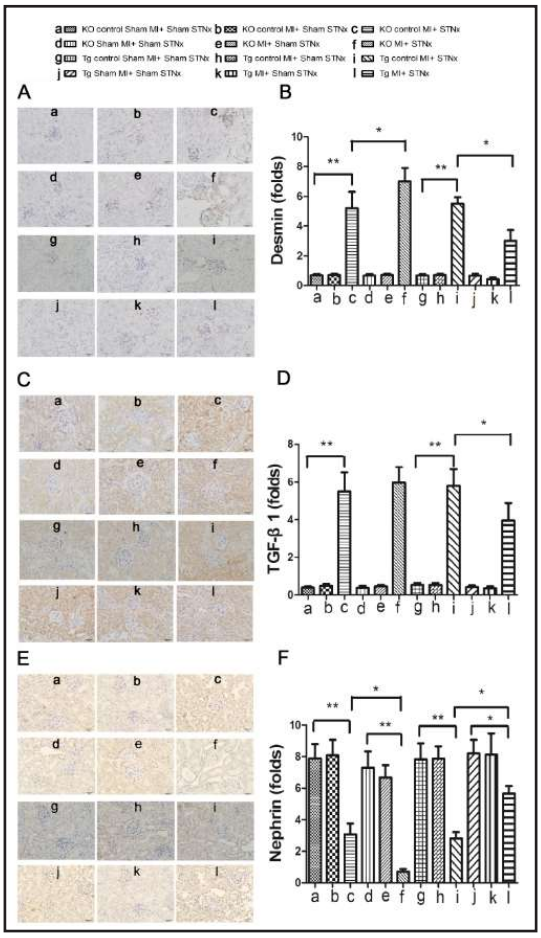

Fig. 5. Effect of SIRT1 on the renal immunohistochemistry and function before and after procedures. A: Immunohistochemistry of Desmin in kidney; B: Desmin score; C: Immunohistochemistry of TGF-β1 in kidney; D: TGF-β1 score; E: Immunohistochemistry of Nephrin in kidney; F: Nephrin score. *P<0.05, ** P<0.01, n=7 for each group.

myocardium had no significant influence on expression of either CHOP or GRP78 (p>0.05, respectively) (Fig. 6 A-D).

In the residual kidney, the CKO group showed significantly higher levels of CHOP, Bax and p53 expression than did the related WT control group (2.64±0.23 vs. 1.74±0.17, P<0.05; 1.49±0.11 vs. 0.96±0.17, P<0.05; 1.84±0.17 vs. 0.77±0.09, P<0.01, respectively) (Fig. 7 A-F), while the SIRT1 overexpression group presented with significantly lower levels of CHOP, Bax, and p53 expression in MI + STNx group than in the Tg control MI + STNx group (1.13±0.19 vs. 1.52±0.13, P<0.05; 0.74±0.12 vs. 1.08±0.24, P<0.05; 0.72±0.10 vs. 0.85±0.19, P<0.05, respectively) (Fig. 7 A- F).

Discussion

Interactions between MI and STNx and their effects on cardiac and renal structure and function

The term "cardio-renal syndrome (CRS)" identifies a disorder of the heart and kidneys whereby acute or chronic dysfunction in one organ may induce acute or chronic dysfunction

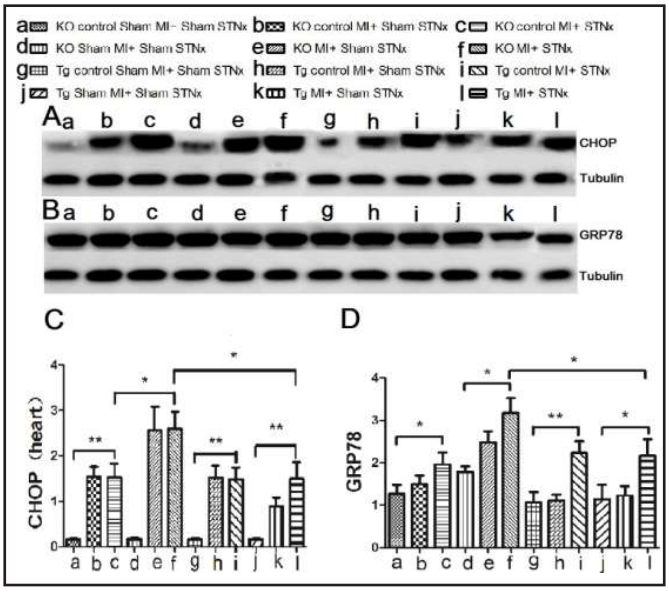

Fig. 6. Representative images of the western blot showing Endoplasmic Reticulum Stress protein expression in the LV tissue from sham MI + sham STNx, MI + sham STNx, and MI + STNx groups in KO and Tg mice. A: CHOP protein expression; B: GRP78 protein expression; C: CHOP protein score; D: GRP78 protein score. *P<0.05, ** P<0.01, n=5 for each group.

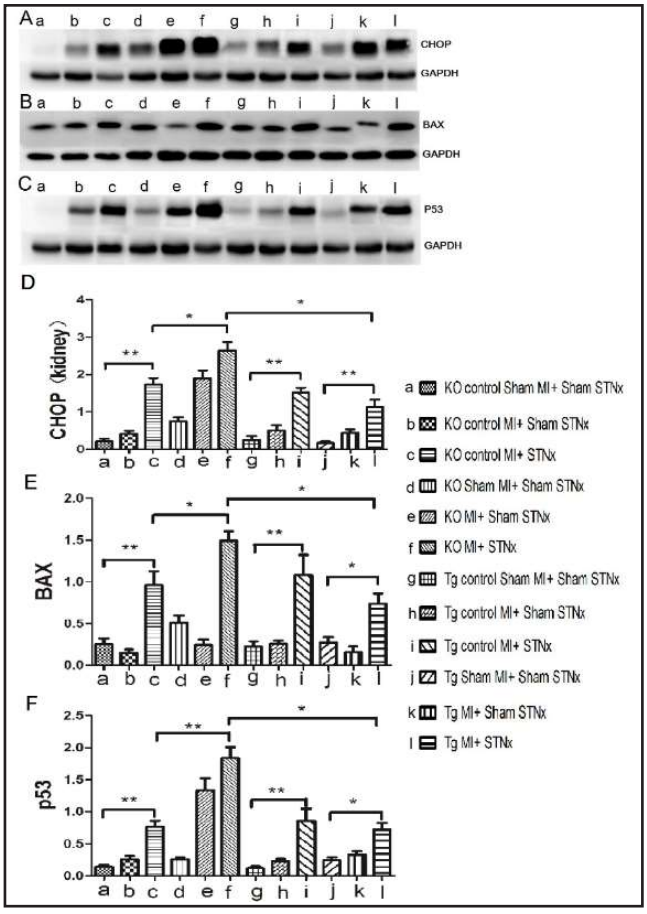

Fig. 7. Representative images of the western blot showing Endoplasmic Reticulum Stress protein expression in the residual kidney tissue from sham MI + sham STNx, MI + sham STNx, and MI + STNx groups in KO and Tg mice. A: CHOP protein expression; B: BAX protein expression; C: p53 protein expression; D: CHOP protein score; E: BAX protein score; F: p53 protein score. *P<0.05, ** P<0.01, n=5 for each group.

in the other organ. Although the current definition of CRS includes five subtypes [23], the subtypes themselves do not indicate the underlying mechanism causing cardiac and/or renal dysfunction. Meanwhile, regarding the effects of MI and/or STNx on the heart and the kidney, conflicting results have been reported by different research groups [2, 24-27].

In the present study, we studied CRS in mice with Sirt1 cardiac-specific knock out or overexpression, and showed that induction of either STNx or MI aggravated structural and functional deterioration of the other organ. These findings reflect the clinical progression of CRS, in which the onset of renal or cardiac dysfunction may worsen the outcome of pre-existing dysfunction of the other organ. However, induction of MI alone did not affect renal structure or function in mice without STNx 28 days post-MI, which might be explained by the relatively preserved EF value in our MI model being insufficient to cause acute or sub-acute renal dysfunction. Likewise, STNx alone had no significant influence on cardiac structure and function, which was in accordance with a previous study in rats [28].

ER stress plays an important role in CRS

Protein synthesis in the ER is of great importance for the normal functioning of both the heart and the kidney [29, 30]. The dysregulation of protein synthesis and/or protein processing within the ER causes the accumulation of unfolded proteins which triggers the unfolded protein response (UPR). The UPR involves multiple mechanisms through which the accumulated unfolded proteins are eliminated, by increasing ER resident chaperones, inhibiting protein translation, and accelerating the clearance of unfolded proteins. However, if ER stress exceeds the capacity of these adaptive mechanisms, the ER initiates apoptotic signaling, which may lead to cell death [31, 32]. Previous studies suggested that ER stress was triggered in diseases affecting either the heart or the kidney, and played a part in the pathological process of these diseases [33-38].

In our present study, induction of either MI or STNx increased expression of GRP78 and CHOP in the associated organ, suggesting that activation of ER stress could underlie the progression of cardiac and renal dysfunction in the settings of CRS. Moreover, induction of MI resulted in higher levels of BAX and CHOP expression in the kidney of mice that had undergone STNx as compared to those that had received MI only, which was in accordance with our previous study in rats [6]. In contrast, within the post-MI myocardium, the mice that underwent STNx presented with higher levels of GRP78 and CHOP expression, as compared to the group that had undergone a sham operation to the kidney. The latter interactions between the heart and the kidney may form a vicious cycle, resulting in significant upregulation of ER stress and subsequent cell death in both organs. However, based on current evidence, we are unsure if the activation of ER stress after stimulus to the other remote organ was merely a manifestation of hemodynamic interactions, or if there were other signal-transduction pathways involved.

Cardiac specific overexpression of SIRT1 modulates ER stress to attenuate post-MI remodeling and improve renal function in CRS

SIRT1 is a member of the Sirtuin family, which is a highly conserved family of histone/protein deacetylases belonging to the class-III group of HDACs [8]. SIRT1 regulates a wide array of cellular processes that are pivotal in the regulation of cellular survival, senescence and metabolism, through deacetylation of a growing list of histones and non-histone proteins [39]. Emerging evidence from *in vitro* and *in vivo* studies indicates that activation of SIRT1 displays pro-survival activity in both the heart and the kidney, and protects both organs from stress [11, 40-44]. In the present study using cardiac-specific SIRT1 knockout and overexpression, we showed that cardiac-specific SIRT1 knockout or overexpression aggravated or attenuated, respectively, the cardiac and renal remodeling/dysfunction in the setting of CRS.

Several studies had demonstrated that activation of SIRT1 attenuates ER stress in both the heart [14, 45] and the kidney [13, 46]. In our current study, cardiac expression of GRP78 and CHOP, and renal expression of CHOP, BAX and p53, were significantly increased in cardiac-specific SIRT1 knockout mice, whereas cardiac-specific SIRT1 overexpression had opposite effects. The latter results indicate that SIRT1 may exert its protective activity through modulation of ER stress in both the heart and the kidney, although the exact underlying mechanism was not investigated. According to previous studies, deacetylation of key transcriptional factors of UPR such as eIF-2αor XBP-1 may be involved [45, 46].

Potential clinical implications

Patients with CKD are frequently excluded from randomized controlled clinical trials of drugs to treat chronic congestive heart failure [47], limiting the evidence on therapeutic efficacy for the management of patients with CRS. Current treatment for chronic heart failure involves many therapeutic approaches that may adversely affect renal function [48]. The present study showed that activation of SIRT1 alleviated both cardiac and renal remodeling/dysfunction in the setting of CRS through modulation of ER stress, indicating that SIRT1 activating compounds such as resveratrol potentially could be used for treatment of CRS.

Limitations

According to previous studies, hemodynamic alternations after induction of MI play a significant part in the progression of CRS [24]. However, in our current study, hemodynamic changes post MI were not restricted, contrasting with previous reports [2]. We observed that induction of either MI or STNx caused activation of ER stress in the other organ. However, based on current evidence, we are unsure if the activation of ER stress after stimulus to the other remote organ was merely a manifestation of hemodynamic interactions, or if there were other signal-transduction pathways involved. Lastly, although our findings indicated that SIRT1 may exert its protective activity through modulation of ER stress in both the heart and the kidney, we did not investigate the exact underlying mechanism(s).

Conclusion

In summary, the present study documented that induction of both MI and STNx aggravated structural and functional deterioration of the other organ, and caused activation of ER stress in both organs. Cardiac-specific knockout of SIRT1 upregulated ER stress in both the heart and the kidney and aggravated cardiac and renal remodeling/dysfunction, whereas cardiac-specific SIRT1 overexpression downregulated ER stress in both organs thereby attenuating cardiac and renal remodeling/dysfunction. The latter findings may shed novel insight into the mechanism underlying interactions between the heart and the kidney in the setting of CRS, and may provide new therapeutic targets.

Acknowledgements

We are grateful to Prof. Wei Zhu of the Second Affiliated Hospital, Zhejiang University School of Medicine, Dr. Jun Xu of Department of Anesthesia, University of Iowa Hospitals and Clinics, Dr. Sarah Poynton of Johns Hopkins University School of Medicine, and Dr. Guangshuo Zhu of Division of Cardiology, Johns Hopkins Medical Institutions for their critical reading and revising of the manuscript.

The present study was supported by a grant from the Science and Technology Commission of Shanghai Municipality (no. 14ZR1432000), and by the grant from National Nature Science Foundation of China (NSFC) (no. 81571363) to Dr. Dong Huang.

Disclosure Statement

The authors have no conflicts of interest relevant to this manuscript.

References

1 Ronco C, Haapio M, House AA, Anavekar N, Bellomo R：Cardiorenal syndrome. J Am Coll Cardiol 2008;52:1527-1539.

2 Rafiq K, Noma T, Fujisawa Y, Ishihara Y, Arai Y, Nabi AH, Suzuki F, Nagai Y, Nakano D, Hitomi H, Kitada K, Urushihara M, Kobori H, Kohno M, Nishiyama A：Renal sympathetic denervation suppresses de novo podocyte injury and albuminuria in rats with aortic regurgitation. Circulation 2012;125:1402-1413.

3 Anand IS, Bishu K, Rector TS, Ishani A, Kuskowski MA, Cohn JN：Proteinuria, chronic kidney disease, and the effect of an angiotensin receptor blocker in addition to an angiotensin-converting enzyme inhibitor in patients with moderate to severe heart failure. Circulation 2009;120:1577-1584.

4 Figueiredo EL, Leao FV, Oliveira LV, Moreira MC, Figueiredo AF：Microalbuminuria in nondiabetic and nonhypertensive systolic heart failure patients. Congestive Heart Failure 2008;14:234-238.

5 Matsushita K：Pathogenetic pathways of cardiorenal syndrome and their possible therapeutic implications. Curr Pharm Des 2016;22:4629-4637.

6 Dong Z, Wu P, Li Y, Shen Y, Xin P, Li S, Wang Z, Dai X, Zhu W, Wei M：Myocardial infarction worsens glomerular injury and microalbuminuria in rats with pre-existing renal impairment accompanied by the activation of er stress and inflammation. Mol Biol Rep 2014;41:7911-7921.

7 Dong Z, Gong K, Huang D, Zhu W, Sun W, Zhang Y, Xin P, Shen Y, Wu P, Li J, Lu Z, Zhang X, Wei M：Myocardial

infarction accelerates glomerular injury and microalbuminuria in diabetic rats via local hemodynamics and immunity. Int J Cardiol 2015;179:397-408.

8 Guarente L. Franklin H：Epstein lecture: Sirtuins, aging, and medicine. N Engl J Med 2011;364:2235-2244.

9 Matsushima S, Sadoshima J：The role of sirtuins in cardiac disease. Am J Physiol Heart Circ Physiol 2015;309:H1375-1389.

10 Alcendor RR, Kirshenbaum LA, Imai S, Vatner SF, Sadoshima J：Silent information regulator 2alpha, a longevity factor and class iii histone deacetylase, is an essential endogenous apoptosis inhibitor in cardiac myocytes. Circ Res 2004;95:971-980.

11 He W, Wang Y, Zhang MZ, You L, Davis LS, Fan H, Yang HC, Fogo AB, Zent R, Harris RC, Breyer MD, Hao CM：Sirt1 activation protects the mouse renal medulla from oxidative injury. J Clin Invest 2010;120:1056-1068.

12 Planavila A, Dominguez E, Navarro M, Vinciguerra M, Iglesias R, Giralt M, Lope-Piedrafita S, Ruberte J, Villarroya F：Dilated cardiomyopathy and mitochondrial dysfunction in sirt1-deficient mice: A role for sirt1-mef2 in adult heart. J Mol Cell Cardiol 2012;53:521-531.

13 Chang JW, Kim H, Baek CH, Lee RB, Yang WS, Lee SK：Up-regulation of sirt1 reduces endoplasmic reticulum stress and renal fibrosis. Nephron 2016;133:116-128.

14 Hsu YJ, Hsu SC, Hsu CP, Chen YH, Chang YL, Sadoshima J, Huang SM, Tsai CS, Lin CY：Sirtuin 1 protects the aging heart from contractile dysfunction mediated through the inhibition of endoplasmic reticulum stress-mediated apoptosis in cardiac-specific sirtuin 1 knockout mouse model. Int J Cardiol 2017;228:543-552.

15 Price NL, Gomes AP, Ling AJ, Duarte FV, Martin-Montalvo A, North BJ, Agarwal B, Ye L, Ramadori G, Teodoro JS, Hubbard BP, Varela AT, Davis JG,Varamini B, Hafner A, Moaddel R, Rolo AP, Coppari R, Palmeira CM, de Cabo R, Baur JA, Sinclair DA：SIRT1 is required for AMPK activation and the beneficial effects of resveratrol on mitochondrial function. Cell Metab 2012;15:675-690.

16 Yamamoto T, Tamaki K, Shirakawa K, Ito K, Yan X, Katsumata Y, Anzai A, Matsuhashi T, Endo J, Inaba T, Tsubota K, Sano M, Fukuda K, Shinmura K：Cardiac Sirt1 mediates the cardioprotective effect of caloric restriction by suppressing local complement system activation after ischemia-reperfusion. Am J Physiol Heart Circ Physiol 2016;15;310:H1003-1014.

17 Ogawa M, Suzuki J, Takayama K, Senbonmatsu T, Hirata Y, Nagai R, Isobe M：Impaired post-infarction cardiac remodeling in chronic kidney disease is due to excessive renin release. Lab Invest 2012;92:1766-1776.

18 Shimazaki M, Nakamura K, Kii I, Kashima T, Amizuka N, Li M, Saito M, Fukuda K, Nishiyama T, Kitajima S, Saga Y, Fukayama M, Sata M, Kudo A：Periostin is essential for cardiac healing after acute myocardial infarction. J Exp Med 2008;205:295-303.

19 Collins KA, Korcarz CE, Lang RM：Use of echocardiography for the phenotypic assessment of genetically altered mice. Physiol Genomics 2003;13:227-239.

20 Sahn DJ, DeMaria A, Kisslo J, Weyman A：Recommendations regarding quantitation in m-mode echocardiography: Results of a survey of echocardiographic measurements. Circulation 1978;58:1072-1083.

21 Kompa AR, Wang BH, Phrommintikul A, Ho PY, Kelly DJ, Behm DJ, Douglas SA, Krum H：Chronic urotensin ii receptor antagonist treatment does not alter hypertrophy or fibrosis in a rat model of pressure-overload hypertrophy. Peptides 2010;31:1523-1530.

22 Rafiq K, Nakano D, Ihara G, Hitomi H, Fujisawa Y, Ohashi N, Kobori H, Nagai Y, Kiyomoto H, Kohno M, Nishiyama A：Effects of mineralocorticoid receptor blockade on glucocorticoid-induced renal injury in adrenalectomized rats. J Hypertens 2011;29:290-298.

23 House AA, Anand I, Bellomo R, Cruz D, Bobek I, Anker SD, Aspromonte N, Bagshaw S, Berl T, Daliento L, Davenport A, Haapio M, Hillege H, McCullough P, Katz N, Maisel A, Mankad S, Zanco P, Mebazaa A, Palazzuoli A, Ronco F, Shaw A, Sheinfeld G, Soni S, Vescovo G, Zamperetti N, Ponikowski P, Ronco C：Definition and classification of cardio-renal syndromes: Workgroup statements from the 7th adqi consensus conference. Nephrol Dial Transplant 2010;25:1416-1420.

24 Lekawanvijit S, Kompa AR, Zhang Y, Wang BH, Kelly DJ, Krum H：Myocardial infarction impairs renal function, induces renal interstitial fibrosis, and increases renal kim-1 expression: Implications for cardiorenal syndrome. Am J Physiol Heart Circ Physiol 2012;302:H1884-1893.

25 Windt WA, Henning RH, Kluppel AC, Xu Y, de Zeeuw D, van Dokkum RP：Myocardial infarction does not further impair renal damage in 5/6 nephrectomized rats. Nephrol Dial Transplant 2008;23:3103-3110.

26 Windt WA, Eijkelkamp WB, Henning RH, Kluppel AC, de Graeff PA, Hillege HL, Schäfer S, de Zeeuw D, van Dokkum RP：Renal damage after myocardial infarction is prevented by renin-angiotensin-aldosterone-

system intervention. J Am Soc Nephrol 2006;17:3059-3066.
27 Bongartz LG, Joles JA, Verhaar MC, Cramer MJ, Goldschmeding R, Tilburgs C, Gaillard CA, Doevendans PA, Braam B：Subtotal nephrectomy plus coronary ligation leads to more pronounced damage in both organs than either nephrectomy or coronary ligation. Am J Physiol Heart Circ Physiol 2012;302:H845-54.
28 Reddy V, Bhandari S, Seymour AM：Myocardial function, energy provision, and carnitine deficiency in experimental uremia. J Am Soc Nephrol 2007;18:84-92.
29 Minamino T, Komuro I, Kitakaze M：Endoplasmic reticulum stress as a therapeutic target in cardiovascular disease. Circ Res 2010;107:1071-1082.
30 Taniguchi M, Yoshida H：Endoplasmic reticulum stress in kidney function and disease. Curr Opin Nephrol Hypertens 2015;24:345-350.
31 Xu C, Bailly-Maitre B, Reed JC：Endoplasmic reticulum stress: Cell life and death decisions. J Clin Invest 2005;115:2656-2664.
32 Ron D, Walter P：Signal integration in the endoplasmic reticulum unfolded protein response. Nat Rev Mol Cell Biol 2007;8:519-529.
33 Dickhout JG, Carlisle RE, Austin RC：Interrelationship between cardiac hypertrophy, heart failure, and chronic kidney disease: Endoplasmic reticulum stress as a mediator of pathogenesis. Circ Res 2011;108:629-642.
34 Petrovski G, Das S, Juhasz B, Kertesz A, Tosaki A, Das DK：Cardioprotection by endoplasmic reticulum stress-induced autophagy. Antioxid Redox Signal 2011;14:2191-2200.
35 Zhang MZ, Wang Y, Paueksakon P, Harris RC：Epidermal growth factor receptor inhibition slows progression of diabetic nephropathy in association with a decrease in endoplasmic reticulum stress and an increase in autophagy. Diabetes 2014;63:2063-2072.
36 Dong G, Liu Y, Zhang L, Huang S, Ding HF, Dong Z：mTor contributes to er stress and associated apoptosis in renal tubular cells. Am J Physiol Renal Physiol 2015;308:F267-274.
37 Dong ZX, Wan L, Wang RJ, Shi YQ, Liu GZ, Zheng SJ, Hou HL, Han W, Hai X：Epicatechin suppresses angiotensin II-induced cardiac hypertrophy via the activation of the SP1/SIRT1 signaling pathway. Cell Physiol Biochem 2017;41:2004-2015.
38 Ruan Y, Dong C, Patel J, Duan C, Wang X, Wu X, Cao Y, Pu L, Lu D, Shen T, Li J：SIRT1 suppresses doxorubicin-induced cardiotoxicity by regulating the oxidative stress and p38MAPK pathways. Cell Physiol Biochem 2015;35:1116-1124.
39 Sundaresan NR, Pillai VB, Gupta MP：Emerging roles of sirt1 deacetylase in regulating cardiomyocyte survival and hypertrophy. J Mol Cell Cardiol 2011;51:614-618.
40 Cheng HL, Mostoslavsky R, Saito S, Manis JP, Gu Y, Patel P, Bronson R, Appella E, Alt FW, Chua KF：Developmental defects and p53 hyperacetylation in sir2 homolog (sirt1)-deficient mice. Proc Natl Acad Sci U S A 2003;100:10794-10799.
41 Alcendor RR, Gao S, Zhai P, Zablocki D, Holle E, Yu X, Tian B, Wagner T, Vatner SF, Sadoshima J：Sirt1 regulates aging and resistance to oxidative stress in the heart. Circ Res 2007;100:1512-1521.
42 Hsu CP, Zhai P, Yamamoto T, Maejima Y, Matsushima S, Hariharan N, Shao D, Takagi H, Oka S, Sadoshima J：Silent information regulator 1 protects the heart from ischemia/reperfusion. Circulation 2010;122:2170-2182.
43 Kume S, Haneda M, Kanasaki K, Sugimoto T, Araki S, Isono M, Isshiki K, Uzu T, Kashiwagi A, Koya D：Silent information regulator 2 (sirt1) attenuates oxidative stress-induced mesangial cell apoptosis via p53 deacetylation. Free Radic Biol Med 2006;40:2175-2182.
44 Fan H, Yang HC, You L, Wang YY, He WJ, Hao CM：The histone deacetylase, sirt1, contributes to the resistance of young mice to ischemia/reperfusion-induced acute kidney injury. Kidney Int 2013;83:404-413.
45 Prola A, Silva JP, Guilbert A, Lecru L, Piquereau J, Ribeiro M, Mateo P, Gressette M, Fortin D, Boursier C, Gallerne C, Caillard A, Samuel JL, Francois H, Sinclair DA, Eid P, Ventura-Clapier R, Garnier A, Lemaire C：Sirt1 protects the heart from er stress-induced cell death through eIF2α deacetylation. Cell Death Differ 2017;24:343-356.
46 Wang FM, Chen YJ, Ouyang HJ：Regulation of unfolded protein response modulator xbp1s by acetylation and deacetylation. Biochem J 2011;433:245-252.
47 Coca SG, Krumholz HM, Garg AX, Parikh CR：Underrepresentation of renal disease in randomized controlled trials of cardiovascular disease. JAMA 2006;296:1377-1384.
48 Longhini C, Molino C, Fabbian F：Cardiorenal syndrome: Still not a defined entity. Clin Exp Nephrol 2010;14:12-21.